Bioorganic & Medicinal Chemistry 17 (2009) 6251–6256

Contents lists available at ScienceDirect

Bioorganic & Medicinal Chemistry

journal homepage: www.elsevier.com/locate/bmc

Tessaric acid derivatives induce G_2/M cell cycle arrest in human solid tumor cell lines

Leticia G. León [a,b], Osvaldo J. Donadel [c,*], Carlos E. Tonn [c], José M. Padrón [a,b,*]

[a] Instituto Universitario de Bio-Orgánica 'Antonio González' (IUBO-AG), Universidad de La Laguna, C/ Astrofísico Francisco Sánchez 2, 38206 La Laguna, Spain
[b] BioLab, Instituto Canario de Investigación del Cáncer (ICIC), C/ Astrofísico Francisco Sánchez 2, 38206 La Laguna, Spain
[c] INTEQUI-CONICET, Facultad de Química, Bioquímica y Farmacia, Universidad Nacional de San Luis, Chacabuco y Pedernera -5700- San Luis, Argentina

ARTICLE INFO

Article history:
Received 6 May 2009
Revised 13 July 2009
Accepted 22 July 2009
Available online 25 July 2009

Keywords:
Sesquiterpenes
Tessaric acid
Antitumor drugs
Cell cycle arrest
Michael acceptors

ABSTRACT

A series of analogs were synthesized in a straightforward manner from naturally available sesquiterpenes ilicic acid and tessaric acid. The in vitro antiproliferative activities were examined in the human solid tumor cell lines A2780, HBL-100, HeLa, SW1573, T-47D and WiDr. The most potent analog induced considerably growth inhibition in the range 1.9–4.5 μM. Cell cycle studies for tessaric acid derivatives indicated a prominent arrest of the cell cycle at the G_2/M phase. Damage to the cells was permanent as determine by the so called 24+24 drug schedule.

1. Introduction

Despite their potential limitations, natural products provide the source of inspiration for the majority of FDA-approved agents and continue to be one of the major sources of inspiration for drug discovery.[1] Natural products and their derivatives are important in the treatment of life-threatening diseases such as cancer.[2] In particular, solid tumors represent the vast majority of cancers (>90%) with high unmet medical needs.

Sesquiterpenes are widely distributed in Nature and have shown to exhibit diverse pharmacological activities including antitumor, antimicrobial, antifeedant, cytotoxic, antibacterial, antifungal, and allergenic contact dermatitic.[3] For instance, the sesquiterpene eremophilane 07H239-A (**1**) isolated from the marine-derived xylariaceous fungus LL-07H239 has shown cytotoxic activity against a panel of human tumor cell lines (mean IC_{50} 3.2 μg/mL). This compound exhibits selectivity for the human peripheral blood T lymphoblast line CCRF-CEM (IC_{50} 0.9 μg/mL).[4]

In addition, the derivatization of natural sesquiterpenes provides a source for new drug discovery. For instance, ilicic aldehyde **2**, obtained by oxidation of naturally occurring eudesmane sesquiterpene ilicic alcohol **3** (Fig. 1), shows a pharmacological cytoprotective effect and significantly prevents the formation of gastric lesions induced by several necrotizing agents. The structure–activity relationship study revealed that the presence of α,β-unsaturated carbonyl groups appears to be responsible for the bioactivity.[5]

In the course of our search of bioactive plant secondary metabolites isolated from species which grow in the central-western semi-arid area of Argentina, we focused our attention in two plants, *Flourensia oolepis* Blake and *Tessaria absinthioides* H. et A. Taking into account the abundance of such secondary metabolites in the plant material, a series of chemical derivatives were prepared.

Within our program directed at the discovery of novel drugs for the treatment of solid tumors, we report on the cytotoxic activity of these compounds against the representative panel of human solid tumor cell lines A2780 (ovarian), HBL-100 (breast), HeLa (cervix), SW1573 (non-small cell lung), T-47D (breast) and WiDr

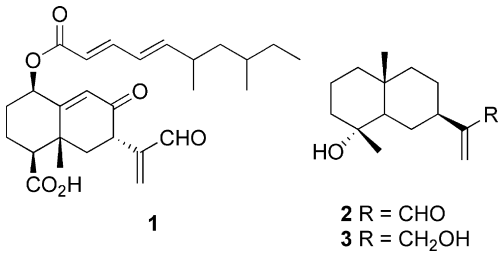

1

2 R = CHO
3 R = CH_2OH

Figure 1. Structures of 07H239-A (**1**), ilicic aldehyde (**2**) and ilicic alcohol (**3**).

* Corresponding authors. Tel.: +34 922316502x6126; fax: +34 922318571.
E-mail addresses: odonadel@unsl.edu.ar (O.J. Donadel), jmpadron@ull.es (J.M. Padrón).

0968-0896/$ - see front matter © 2009 Elsevier Ltd. All rights reserved.
doi:10.1016/j.bmc.2009.07.053

(colon). In addition, cell cycle studies were carried out with the most active derivatives.

2. Results and discussion

2.1. Synthesis

From *F. oolepis* Blake,[6] we obtained the metabolites ilicic alcohol (**3**) and ilicic acid (**4**). The oxidation of ilicic alcohol (**3**) with Jones reagent afforded ilicic aldehyde (**2**) as reported earlier.[5] Ilicic acid (**4**) was the starting material to prepare the set of derivatives **5**-**7** (Scheme 1). The dehydration under acid conditions of **4** led to compound **5** in 55% yield.[7] Direct esterification with MeOH/HCl of **4** and **5** afforded in high yields the corresponding methyl ester derivatives **6** and **7**, respectively.

From *T. absinthioides* H. et A. the eremophilane tessaric acid (**8**) was isolated.[8] As shown in Scheme 2, methyl ester derivative **9** was obtained from **8** by direct esterification under standard conditions. Subsequent reduction of the ketone group with $LiAlH_4$ gave allylic alcohol **10** in high yields. To our surprise, the reduction took place in a regioselective manner. None of the primary allylic alcohol was detected. The result is consistent with the previous observation of a similar regioselective tandem reduction–dehydration of compound **8** to afford a conjugated diene on ring A.[5]

To determine the absolute configuration of the hydroxyl group in compound **10**, we performed diverse NMR experiments (Supplementary data). The data showed that the reducing agent attacked through the α face (Fig. 2). Therefore, the absolute stereochemistry of the secondary hydroxyl group of compound **10** was established as *R*.

2.2. Antiproliferative activity

The in vitro antiproliferative activity of compounds **2**-**10** was evaluated using the National Cancer Institute (NCI) protocol[9] after 48 h of drug exposure using the sulforhodamine B (SRB) assay.[10] The results are shown in Table 1. From the GI_{50} values some structure–activity relationships can be inferred. The antiproliferative data reveal that ilicic alcohol (**3**) and all compounds bearing a carboxylic acid group, that is, **4**–**5** and **8**, are inactive against all cell lines. On the contrary, ilicic aldehyde (**2**) and the methyl ester derivatives **7** and **9**–**10** show activity against all cell lines, with GI_{50} values in the range 1.9-38 μM. The odd compound to this trend is methyl ester **6**, which is slightly active only against HBL-100 cells and inactive against all the other cell lines. Interestingly, the dehydration of the tertiary alcohol group of compound **6** produces the more active derivative **7**.

The most active compound of the series is methyl ester **9**, which has two α,β-unsaturated functional groups. The GI_{50} values against all cell lines are in the range 1.9-4.5 μM. The reduction of the ketone group of compound **9** to give derivative **10** induces a slight decrease in biological activity, with GI_{50} values rising to 5.0-29 μM. From these results, it seems that the presence of the α,β-unsaturated ketone improves the cytotoxicity. We speculate that the biological activity of these molecules is provided by the α,β-unsaturated ester located on the side chain.

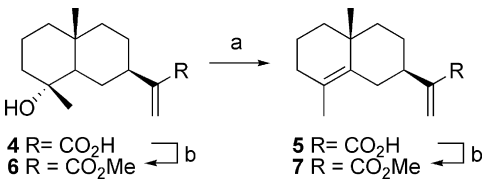

Scheme 1. Reagents and conditions: (a) TsOH, C_6H_6, MS 4 Å, 80 °C, 55%; (b) CH_2N_2, Et_2O, 82% for **6** and 86% for **7**.

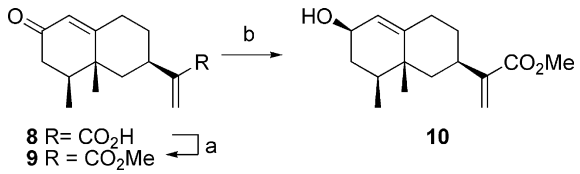

Scheme 2. Reagents and conditions: (a) CH_2N_2, Et_2O, 79%; (b) $LiAlH_4$, THF, 0 °C, 25 min, 83%.

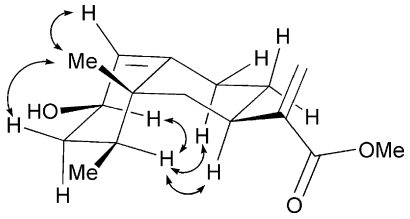

Figure 2. Summary of NOESY experiments.

2.3. 2D-QSAR studies

In order to correlate the observed biological activity (expressed as pGI_{50}, i.e., $-\log GI_{50}$) with the molecular structures of the tested compounds **2**–**10**, we performed a preliminary two-dimensional quantitative structure–activity relationship (2D-QSAR) study. Online software E-DRAGON[11] was used to calculate six molecular descriptors: octanol–water partition coefficient (ALOGP); topological polar surface area (TPSA); molar refractivity (AMR); atomic polarizabilities (Sp); number of H-bonds donor atoms (nHDon); and number of H-bonds acceptor atoms (*n*HAcc). Accordingly, the length of the polynomial regression equation was fixed to seven terms including a constant. With all these data in hand, a 2D-QSAR was performed using multiple linear regression (MLR) method.

Taken as a whole, the results showed modest correlation between pGI_{50} and the descriptors, with squared correlation coefficient (r^2) below 0.87. Hence, we decided to divide the compounds in two groups according to their origin. A first set was comprised of *Fluorensia* derivatives (**2**–**7**), whereas the second included all *Tessaria* derived products (**8**–**10**). The regression coefficients (m_i and b) obtained for both series of compounds against each cell line are presented in Table 2. The residuals (actual–predicted activity) were found to be minimal (Supplementary data). The coefficient r^2 was 1 for all MLR, indicating a perfect correlation between the biological activity and the molecular descriptors. However, this correlation did not allow computing statistical parameters such as *F*-test (degrees of freedom = 0).

The most relevant outcome of the 2D-QSAR study is the dissimilar influence in antiproliferative activity of the molecular parameters for both set of compounds. The activity of derivatives from the *Fluorensia* series was only independent of the number of H-bond acceptors present in the molecule. In contrast, for the *Tessaria* series a correlation was obtained with TPSA and AMR.

2.4. Cell cycle disturbances

When exposed to cytotoxic agents, damaged cells may suffer a stop in their cell cycle. If the cell cannot recover from the damage, cell death occurs through apoptosis. This stop in cell division is known as cell cycle arrest and can occur at any of the cell cycle phases, namely G_0/G_1, S, or G_2/M phase. We studied cell cycle phase distribution by flow cytometry to determine if cell growth inhibition involved cell cycle changes. For these studies we selected ilicic aldehyde (**2**), the most active compound from the *F.*

Table 1
In vitro antiproliferative activity against a representative panel of human solid tumor cell lines[a]

Compound	Cell line					
	A2780 (ovarian)	HBL-100 (breast)	HeLa (cervix)	SW1573 (NSCLC)	T-47D (breast)	WiDr (colon)
2	1.8 (±0.5)	2.8 (±0.5)	16 (±2.4)	2.0 (±0.8)	6.5 (±1.3)	12 (±0.2)
3	>100	>100	>100	>100	>100	>100
4	>100	>100	>100	>100	>100	>100
5	>100	>100	>100	>100	>100	>100
6	>100	74 (±5.1)	>100	>100	>100	>100
7	18 (±0.3)	14 (±1.2)	13 (±3.8)	18 (±3.0)	35 (±15)	38 (±14)
8	>100	>100	>100	>100	>100	>100
9	1.9 (±0.7)	2.4 (±0.8)	4.5 (±1.0)	3.8 (±1.2)	2.4 (±0.7)	2.0 (±0.9)
10	11 (±1.0)	12 (±1.8)	29 (±2.5)	5.0 (±1.0)	11 (±2.9)	17 (±4.2)
5-FU	4.4 (±0.6)	5.5 (±2.3)	19 (±1.2)	4.1 (±0.6)	29 (±2.3)	50 ± (7.2)
CPT	0.46 ± (0.06)	0.23 (±0.05)	1.3 (±0.9)	0.21 (±0.05)	1.9 (±0.4)	1.7 (±0.6)

[a] Values expressed as GI_{50} (50% growth inhibition) are given in μM and are means of two to four experiments, standard deviation is given in parentheses.

Table 2
Results of 2D-QSAR equations obtained by multiple linear regression method[a]

Series	Regression coefficients for descriptors							
	Cell line	m_1 (ALOG)	m_2 (TPSA)	m_3 (AMR)	m_4 (Sp)	m_5 (nHDon)	m_6 (*n*HAcc)	*b*
Fluorensia (**2-7**)	A2780	44.69187383	0.685780741	−31.58107228	73.7	−17.22406152	0	200.5219041
	HBL-100	43.894381	0.673865893	−31.00322064	72.4	−16.95739442	0	195.6905551
	HeLa	54.54797646	0.809939073	−37.66338488	88.3	−19.42647019	0	222.6198786
	SW1573	44.80476696	0.691015265	−31.77496727	74.1	−17.4739903	0	203.7655081
	T-47D	29.01555882	0.449349722	−20.63769208	48.1	−11.4250952	0	134.8179856
	WiDr	27.01167537	0.41376173	−19.06398435	44.5	−10.36758988	0	122.2105189
Tessaria (**8**–**10**)	A2780	0	−0.218548534	−0.136723396	0	0	0	25.43439044
	HBL−100	0	−0.198136989	−0.115434447	0	0	0	22.83730484
	HeLa	0	−0.205471457	−0.190645006	0	0	0	28.49051516
	SW1573	0	−0.075457655	0.127063492	0	0	0	−0.774404025
	T-47D	0	−0.185274203	−0.087023744	0	0	0	20.15309827
	WiDr	0	−0.250112433	−0.212463151	0	0	0	32.44192614

[a] Polynomial regression equation in the form $pGI_{50} = m_1 \times ALOG + m_2 \times TPSA + m_3 \times AMR + m_4 \times Sp + m_5 \times nHDon + m_6 \times nHAcc + b$.

oolepis Blake series. From the *T. absinthioides* H. et A. derivatives we studied methyl esters **9** and **10** in order to detect possible differences due to the presence of one or two α,β-unsaturated carbonyls.

The effect on the cell cycle was investigated in the six human solid tumor cell lines after 24 h exposure. Cells were exposed to each compound at two different drug concentrations (high and low). The drug doses were chosen based on two premises.[12] On the one hand, the GI_{50} values against each cell line. On the other hand, the sensitivity of the cell line to drug treatment, since at higher drug doses large cell death prevents examination of the cell cycle phase distribution. Therefore, the cells were exposed to 5 (low) and 20 μM (high) of ilicic aldehyde (**2**), to 3 (low) and 6 μM (high) of methyl ester **9**, and 15 (low) and 35 μM (high) of methyl ester **10**. Control cells were incubated in the absence of test drug.

Overall, the tested compounds induced cell cycle arrest in the S or G_2/M phases in all cell lines and in a dose dependent manner. However, the results of cell cycle distributions of samples collected from control and treated cells show a diverse pattern of activity. Ilicic aldehyde (**2**) produced a minor arrest in S or G_2/M phase (data not shown). Remarkable results were obtained for the ester derivatives **9** and **10** against the more resistant[13] cell lines HeLa, SW1573, T-47D and WiDr (Fig. 3). When the cervix and lung cancer cells were treated at a low drug concentration a similar level of arrest in the G_2/M phase was observed for derivatives **9** and **10**. This increase was concomitant with a decrease in the S compartment. However, at the high drug dose accumulation in both the S and G_2/M phases was observed. Concomitant with this increase was a parallel decrease in the percentage of cells in the G_0/G_1 phase. In T-47D and WiDr cells, the cell cycle arrest was more prominent in the G_2/M phase compartment (Fig. 4). Concomitant with this increase in the percentage of cells in the G_2/M phase was a parallel decrease in the percentage of cells in the G_0/G_1 and S phases.

Although it is widely acknowledged that nonspecific covalent binding should be avoided in drug development, medicinal chemistry strategies that enable rational approaches to therapeutics that bind through targeted covalent interactions have proven valid.[14] In addition, there are a number of covalent modifiers in preclinical or early clinical investigation that will continue to offer insight to this drug discovery strategy. Earlier, we have used this strategy to prepare a set of cytotoxic compounds containing an α,β-unsaturated carbonyl group, a so called Michael acceptor.[15] Michael acceptors constitute a framework that can bind covalently to nucleophiles inside the cell and consequently, a permanent damage to cells is likely to occur.

The compounds evaluated in this study possess at least one α,β-unsaturated carbonyl group. Therefore, we exposed cells to drugs **9** and **10** for a 24 h period, after which time the drug was washed away and cells were kept in a drug free medium for an additional period of 24 h, the so-called 24+24 drug schedule. Cells were then collected and their cell cycle distribution was examined. The drug doses chosen for these experiments were 3 (low) and 6 μM (high) for methyl ester **9**, and 15 (low) and 35 μM (high) for methyl ester **10**. Figure 5 shows the effect of the 24+24 drug schedule against T-47D and WiDr cells. Overall, compounds **9** and **10** induced damage to all cell lines, which was persistent after the drug was washed away and cells had a 24 h period to recover. The effect was observed by an increase of the Sub G_0 compartment, denoting cell death (Fig. 5c and d).

A major drawback of the current available anticancer drugs is their relative expensive chemical synthesis. This inconvenient

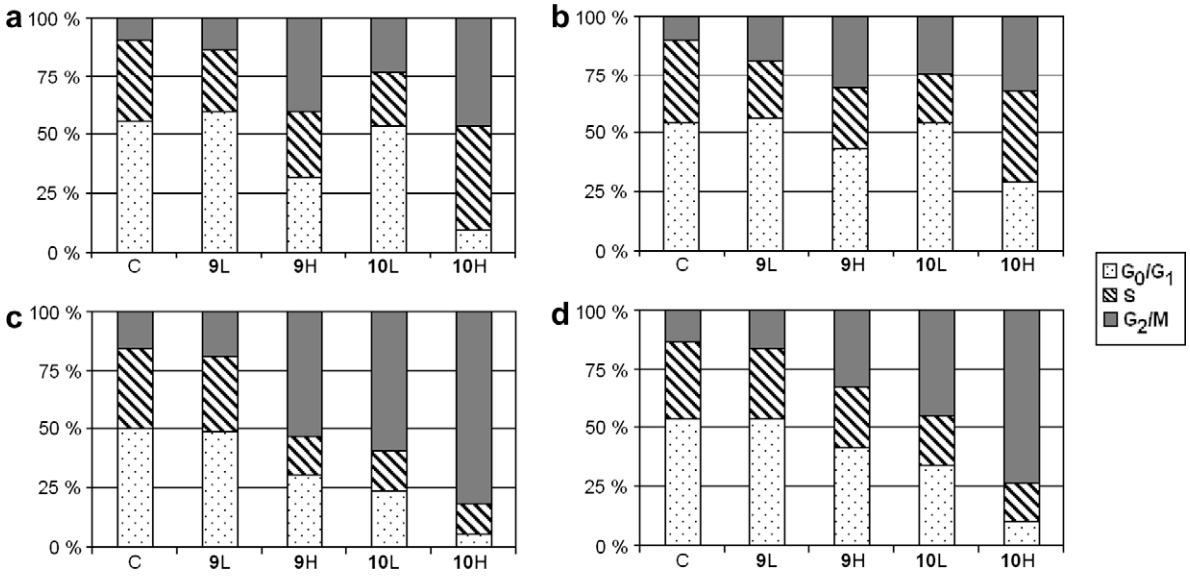

Figure 3. Cell cycle phase distribution in untreated cells (C) and cells treated with compounds **9** and **10**, for 24 h at low (L) and high (H) dose concentrations; (a) HeLa, (b) SW1573, (c) T-47D and (d) WiDr.

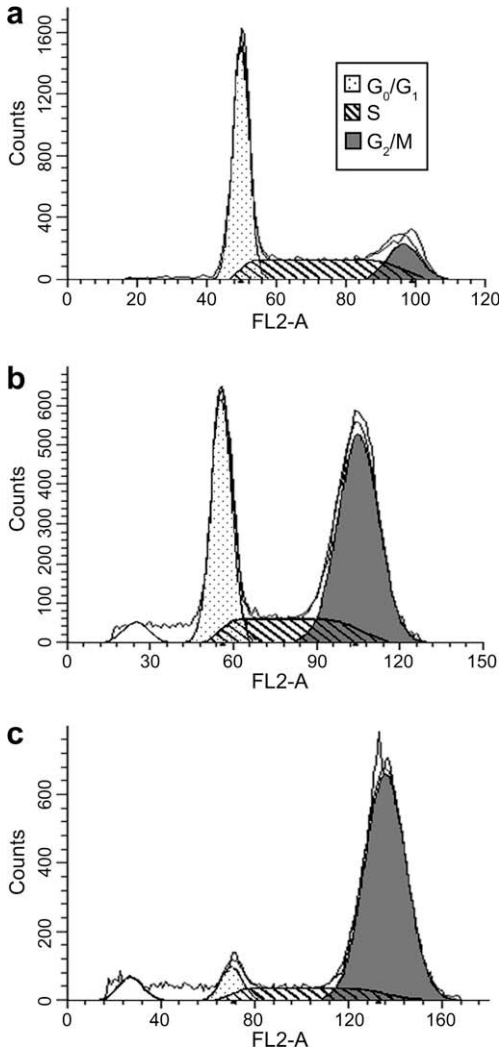

Figure 4. Histogram of T-47D cells after exposure to analogues **9** and **10** for 24 h. (a) control; (b) compound **9** at 6 μM; (c) compound **10** at 35 μM.

can be circumvented by the use of natural products present in large amounts in plants. The goal lies in finding the appropriate modifications in few chemical steps to obtain new derivatives with improved pharmacological activity. We have shown recently how to activate natural products to obtain readily easy antiproliferative and cytotoxic analogs.[16] Thus, natural products may serve not only as potential drugs but as templates to design new drugs.

In conclusion, we have synthesised a set of derivatives from readily available natural products. The in vitro antiproliferative data showed the relevance of the chemical derivatization in order to obtain active products. Cell cycle studies indicated a clear G_2/M phase arrest for the most active compounds. Damage to the cells was permanent as determine by the so called 24+24 drug schedule. Optimized anticancer activities should rise from the preparation of novel analogs taking compound **9** as the lead. Although the mechanism of action is unknown, further studies are being conducted to identify the exact cellular target and will be reported elsewhere.

3. Experimental

3.1. General

All starting materials were commercially available research-grade chemicals and used without further purification. RPMI 1640 medium was purchased from Flow Laboratories (Irvine, UK), fetal calf serum (FCS) was from Gibco (Grand Island, NY), trichloroacetic acid (TCA) and glutamine were from Merck (Darmstadt, Germany), and penicillin G, streptomycin, dimethyl sulfoxide (DMSO) and sulforhodamine B (SRB) were from Sigma (St Louis, MO).

3.2. Preparation, physical and spectroscopic data of the compounds

3.2.1. General method for the esterification of carbolxylic acids

To a solution of acid (1 mmol) in 50 mL of dry ether an ethereal diazomethane solution was added dropwise until a yellow color persisted. TLC showed reaction completion. Then, the solvent was evaporated at reduced pressure. Flash chromatography on silica gel (hexane/EtOAc 9:1) afforded the corresponding ester.

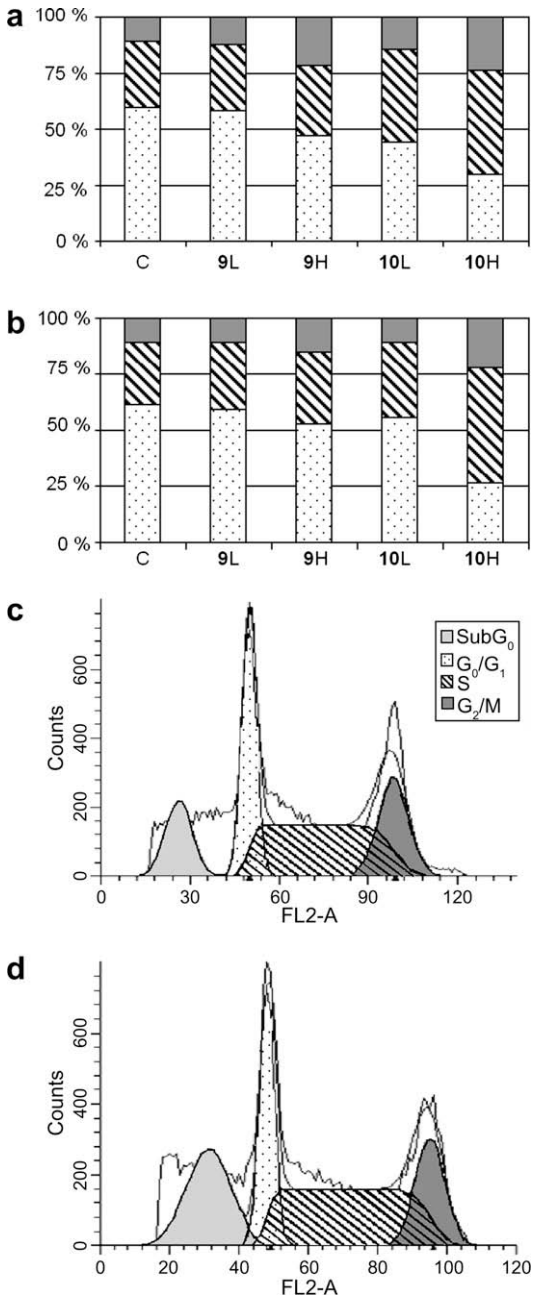

Figure 5. Representative results of drug schedule 24+24. Cell cycle phase distribution in untreated cells (C) and cells treated with compounds **9** and **10**, at low (L) and high (H) dose concentrations; (a) T-47D and (b) WiDr. Histogram of cells after exposure to analog **10** at 35 μM: (c) T-47D; (d) WiDr.

3.2.2. γ-Costic acid. 2-((2*R*,4a*R*)-4a,8-dimethyl-1,2,3,4,4a,5,6,7-octahydronaphthalen-2-yl)acrylic acid (5)

Compound **5** was obtained according known procedures.[7] ^{1}H NMR ($CDCl_3$, TMS, 200 MHz), δ (ppm): 6,37 (s, 1H), 5,71 (s, 1H), 3.75 (s, 3H), 2.63 (ddd, 1H), 2,42 (m, 1H), 1.95 (m, 2H), 1.61 (s, 1H), 1,07 (s, 1H), ^{13}C NMR ($CDCl_3$, 50.25 MHz) δ: 167.8, 145.6, 134.24, 125.08, 122.46, 122.36, 51.68, 42.06, 40.51, 40.10, 34.36, 33.05, 31.32, 27.96, 24.54, 19.24, 10.0. HRMS (EI$^+$) calcd for $C_{15}H_{22}O_2$ [M$^+$] 234.1619, found 234.

3.2.3. Ilicic acid methyl esther. Methyl 2-((2*R*,4a*R*,8*R*)-8-hydroxy-4a,8-dimethyl-decahydronaphthalen-2-yl)acrylate (6)

The general esterification method was applied to ilicic acid (**4**, 500 mg, 1.98 mmol) to give compound **6** as a yellow oil (404 mg, 76%). $[\alpha]_D^{29}$ −35.8 (*c* 1, $CHCl_3$); IR (KBr, cm^{-1}): 3450, 1710, and 1620 cm^{-1}; ^{1}H NMR ($CDCl_3$, TMS, 200 MHz), δ (ppm): 6.09 (d, *J* = 1.5 Hz, 1H), 5.51 (s, 1H), 3.70 (s, 3H), 1.07 (s, 3H), 0.86 (s, 3H). ^{13}C NMR ($CDCl_3$, 50.25 MHz) δ: 167.71, 145.41, 122.38, 72.14, 54.69, 51.58, 44.25, 43.11, 40.67, 40.16, 34.38, 27.05, 26.21, 22.21, 19.87, 18.48. Anal. Calcd for $C_{16}H_{24}O_2$: 72.14; H, 9.84; 0, 18.02. Found: C. 71.95; H, 9.97; 0, 18.35.

3.2.4. γ-Costic acid methyl esther. Methyl 2-((2*R*,4a*R*)-4a,8-dimethyl-1,2,3,4,4a,5,6,7-octahydronaphthalen-2-yl)acrylate (7)

The general esterification method was applied to γ-costic acid (**5**, 500 mg, 2.13 mmol) to give compound **7** as an oil (428 mg, 81%). ^{1}H NMR ($CDCl_3$, TMS, 200 MHz), δ (ppm): 6.15 (s, 1H), 5.56 (s, 1H), 3.75 (br s, 1H), 1.05 (s, 3H), 1.60 (s, 3H), 2.65 (d, 1H), 1.69 (br s, 1H), 2.40 (m, 1H), 1.75–1.44 (m, 2H). ^{13}C NMR ($CDCl_3$, 50.25 MHz) δ: 167.80, 142.62, 134.24, 125.08, 122.26, 51.68, 42.07, 41.50, 40.10, 34.37, 33.04, 31.32, 27.96, 24.54, 19.24, 19.00. MS (EI$^+$) calcd for $C_{16}H_{24}O_2$ [M$^+$] 248.36, found 248.

3.2.5. Tessaric acid methyl esther. Methyl 2-((2*R*,8*S*,8a*R*)-8,8a-dimethyl-6-oxo-1,2,3,4,6,7,8,8a-octahydronaphthalen-2-yl)acrylate (9)

The general esterification method was applied to tessaric acid (**8**, 500 mg, 2.02 mmol) to give compound **9** as a yellow oil (417 mg, 79%). ^{1}H NMR ($CDCl_3$, TMS, 200 MHz), δ (ppm): 3.76 (s, 3H), 1.06 (s, 3H), 0.97 (s, *J* = 8 Hz 3H), 6.19 (s, 1H), 5.57 (s, 1H), 5.86 (s, 1H), 2.58 (m, 1H), 1.55 (dd, *J* = 6,6′ = 6,7 = 6′,7 = 14 Hz, 1H), 1.72-1.86 (m, 1H). ^{13}C NMR ($CDCl_3$, 50.25 MHz) δ: 199.5, 173.86, 167.39, 144.25, 125.65, 123.15, 42.00, 40.26, 39.4, 35.81, 32.63, 29.18, 28.85, 19.02, 15.34. 51.86 (OMe). MS (EI$^+$) calcd for $C_{16}H_{24}O_2$ [M$^+$] 262.34, found 262.

3.2.6. Methyl 2-((2*R*,6*R*,8*S*,8a*R*)-6-hydroxy-8,8a-dimethyl-1,2,3,4,6,7,8,8a-octahydronaphthalen-2-yl)acrylate (10)

To a stirred solution of **9** (327 mg, 1.25 mmol) in dry THF (10 mL) in an ice-cold bath was added slowly $LiAlH_4$ (69 mg, 1.88 mmol). After 25 min to the reaction mixture H_2O (70 μL), 15% NaOH aqueous solution 70 μL) and H_2O (2.7 mL) were sequentially added with stirring. The mixture was allowed to reach rt, dried over $MgSO_4$, filtered through a pad of celite, concentrated, and purified by silica gel column chromatography, to yield **10** (273 mg, 83% yield) as an oil. $[\alpha]_D^{20}$ −59.8 (*c* 1, $CHCl_3$); ^{1}H NMR ($CDCl_3$, TMS, 200 MHz), δ (ppm): 6.12 (s, 1H), 5.54 (s, 1H) y 5.42 (s, 1H), 4.27 (m, 1H), 0.93 (s, 3H), 0.87 (d, *J* = 8.0 Hz, 3H). ^{13}C NMR ($CDCl_3$, 50.25 MHz) δ: 167.61, 148.89, 145.03, 122.53, 119.82, 96.08, 71.52, 40.35, 35.74, 32.85, 32.63, 29.68, 26.07, 21.47, 15.65, 51.69 (OMe). MS (EI$^+$) calcd for $C_{16}H_{24}O_3$ [M$^+$] 264.04, found 264. Anal. Calcd for $C_{16}H_{24}O_3$: C, 72.69; H, 9.15; O, 18.16. Found: C, 72.63; H, 9.01; O, 18.36.

3.3. 2D-QSAR studies

All computational studies were performed using E-DRAGON (VCCLAB, Virtual Computational Chemistry Laboratory, http://www.vcclab.org, 2005),[11] the electronic remote version of the application for the calculation of molecular descriptors DRAGON. Six descriptors were used in this study: ALOGP, Ghose-Crippen octanol–water partition coefficient (log *P*); TPSA, topological polar surface area; AMR, molar refractivity; Sp, sum of atomic polarizabilities (scaled on Carbon atom); nHDon, number of donor atoms for H-bonds; and *n*HAcc, number of acceptor atoms for H-bonds. Molecular structure files with 3D optimized structures were obtained on-line using CORINA, provided by Molecular Networks GMBH (http://www.molecular-networks.com/). Multiple linear regression (MLR) was performed with Microsoft® Office Excel® 2007 (Microsoft Corporation, WA, USA).

3.4. Biological tests

3.4.1. Cells, culture and plating

The human solid tumor cell lines A2780, HBL-100, HeLa, SW1573, WiDr and T-47D were used in this study. Cells were maintained in 25 cm^2 culture flasks in RPMI 1640 supplemented with 5% heat inactivated fetal calf serum and 2 mM L-glutamine in a 37 °C, 5% CO_2, 95% humidified air incubator. Exponentially growing cells were trypsinized and resuspended in antibiotic containing medium (100 units penicillin G and 0.1 mg of streptomycin per mL). Single cell suspensions displaying >97% viability by trypan blue dye exclusion were subsequently counted. After counting, dilutions were made to give the appropriate cell densities for inoculation onto 96-well microtiter plates. Cells were inoculated in a volume of 100 μL per well at densities of 15,000 (WiDr, T-47D and HeLa) and 10,000 (A2780, SW1573 and HBL-100) cells per well, based on their doubling times.

3.4.2. Antiproliferative tests

Chemosensitivity tests were performed using the SRB assay of the NCI with slight modifications. Briefly, pure compounds were initially dissolved in DMSO at 400 times the desired final maximum test concentration. Control cells were exposed to an equivalent concentration of DMSO (0.25% v/v, negative control). Each agent was tested in triplicates at different dilutions in the range 1–100 μM. The drug treatment was started on day 1 after plating. Drug incubation times were 48 h, after which time cells were precipitated with 25 μL ice-cold 50% (w/v) trichloroacetic acid and fixed for 60 min at 4 °C. Then the SRB assay was performed. The optical density (OD) of each well was measured at 492 nm, using BioTek's PowerWave XS Absorbance Microplate Reader. Values were corrected for background OD from wells only containing medium. The percentage growth (PG) was calculated with respect to untreated control cells (C) at each of the drug concentration levels based on the difference in OD at the start (T_0) and end of drug exposure (T), according to NCI formulas. Therefore, if T is greater than or equal to T_0 the calculation is $100 \times [(T - T_0)/(C - T_0)]$. If T is less than T_0 denoting cell killing the calculation is $100 \times [(T - T_0)/(T_0)]$. The effect is defined as percentage of growth, where 50% growth inhibition (GI_{50}) represents the concentration at which PG is +50. With these calculations a PG value of 0 corresponds to the amount of cells present at the start of drug exposure, while negative PG values denote net cell kill.

3.4.3. Cell-cycle analysis

Cells were seeded in a six well plates at a density of 2.5–5×10^5 cells/well. After 24 h the products were added to the respective well and incubated for an additional period of 24 h. Cells were trypsinized, harvested, transferred to test tubes (12×75 mm) and centrifuged at 1500 rpm for 10 min at 5 °C. The supernatant was discarded and the cell pellets were resuspended in 200 μL of cold PBS and fixed by the addition of 1 mL ice-cold 70% ethanol. Fixed cells were incubated overnight at –20 °C after which time was centrifuged at 1500 rpm for 10 min. The cell pellets were resuspended in 500 μL PBS. Then, 5 μL of DNAse-free RNAse (10 mg/mL) was incubated in the dark at 37 °C for 30 min. After incubation 5 μL of propidium iodide (0.5%) was added. Flow cytometric determination of DNA content (25,000 cells/sample) was analyzed by FACSCalibur Flow Cytometer (Becton Dickinson, San José, CA, USA). The fractions of the cells in G_0/G_1, S, and G_2/M phase were analyzed using cell cycle analysis software, ModFit LT 3.0 (Verity Software House, Topsham, ME, USA).

Acknowledgments

This research was supported by CONICET (PIP 112-200801-00628), UNSL (Project 7301), the Spanish MICIIN (CTQ2008-06806-C02-01/BQU) and the Canary Islands Agencia Canaria de Investigación, Innovación y Sociedad de la Información (PI 2007/021) co-financed by the European Social Fund (FEDER), the Spanish MSC (RTICC RD06/0020/1046) and FUNCIS (PI 01/06 and 35/06). L.G.L. thanks the Spanish MSC-FIS for a postdoctoral contract. J.M.P. thanks the Spanish MEC-FSE for a Ramón y Cajal contract.

Supplementary data

Supplementary data associated with this article can be found, in the online version, at doi:10.1016/j.bmc.2009.07.053.

References and notes

1. (a) Newman, D. J. *J. Med. Chem.* **2008**, *51*, 2589; (b) Newman, D. J.; Cragg, G. M. *J. Nat. Prod.* **2007**, *70*, 461.
2. Butler, M. S.; Newman, D. J. *Prog. Drug. Res.* **2008**, *65*, 3.
3. Picman, A. K. *Biochem. Syst. Ecol.* **1986**, *14*, 256.
4. McDonald, L. A.; Barbieri, L. R.; Bernan, V. S.; Janso, J.; Lassota, P.; Carter, G. T. *J. Nat. Prod.* **2004**, *67*, 1565.
5. Donadel, O. J.; Guerreiro, E.; María, A. O.; Wendel, G.; Enriz, R. D.; Giordano, O. S.; Tonn, C. E. *Bioorg. Med. Chem. Lett.* **2005**, *15*, 3547.
6. Guerreiro, E.; Kavka, J.; Giordano, O. S.; Gros, E. G. *Phytochemistry* **1979**, *18*, 1235.
7. (a) Donadel, O. J.; García, E. E.; Guerreiro, E.; Tonn, C. E. *An. Asoc. Quim. Argent.* **1998**, *86*, 90; (b) Donadel, O. J.; Guerreiro, E.; Ardanaz, C. E. *Rapid Commun. Mass Spectrom.* **2001**, *15*, 164.
8. Kurina Sanz, M. B.; Donadel, O. J.; Rossomando, P. C.; Tonn, C. E.; Guerreiro, E. *Phytochemistry* **1997**, *44*, 897.
9. Skehan, P.; Storeng, P.; Scudeiro, D.; Monks, A.; McMahon, J.; Vistica, D.; Warren, J. T.; Bokesch, H.; Kenney, S.; Boyd, M. R. *J. Natl. Cancer Inst.* **1990**, *82*, 1107.
10. Miranda, P. O.; Padrón, J. M.; Padrón, J. I.; Villar, J.; Martín, V. S. *ChemMedChem* **2006**, *1*, 323.
11. Tetko, I. V.; Gasteiger, J.; Todeschini, R.; Mauri, A.; Livingstone, D.; Ertl, P.; Palyulin, V. A.; Radchenko, E. V.; Zefirov, N. S.; Makarenko, A. S.; Tanchuk, V. Y.; Prokopenko, V. V. *J. Comput. Aid. Mol. Des.* **2005**, *19*, 453.
12. Padrón, J. M.; Peters, G. J. *Invest. New Drugs* **2006**, *24*, 195.
13. Pizao, P. E.; Peters, G. J.; van Ark-Otte, J.; Smets, L. A.; Smitskamp-Wilms, E.; Winograd, B.; Pinedo, H. M.; Giaccone, G. *Eur. J. Cancer* **1993**, *29A*, 1566.
14. Potashman, M. H.; Duggan, M. E. *J. Med. Chem.* **2009**, *52*, 1231.
15. León, L. G.; Carballo, R. M.; Vega-Hernández, M. C.; Miranda, P. O.; Martín, V. S.; Padrón, J. I.; Padrón, J. M. *ChemMedChem* **2008**, *3*, 1740.
16. (a) Córdova, I.; León, L. G.; León, F.; San Andrés, L.; Luis, J. G.; Padrón, J. M. *Eur. J. Med. Chem.* **2006**, *41*, 1327; (b) Pungitore, C. R.; León, L. G.; García, C.; Martín, V. S.; Tonn, C. E.; Padrón, J. M. *Bioorg. Med. Chem. Lett.* **2007**, *17*, 1332.